Temporal and spatial scales of Near-Intertial Oscillations inferred from surface drifters.

Hélène Etienne[1], Clément Ubelmann[2], Fabrice Ardhuin[3], Gérald Dibarboure[4]

5 [1]Collecte Localisation Satellite, Ramonville Saint-Agne, France
[2]Datlas, Grenoble, France
[3]Laboratoire d'Océanographie Physique et Spatiale, Centre National de la Recherche Scientifique – Ifremer, Plouzané, France
[4]Centre National d'Etudes Spatiales, Toulouse, France

10 *Correspondence to*: Hélène Etienne (hetienne@groupcls.com)

Abstract.

The study investigates near-inertial oscillations (NIOs) in ocean surface currents, which are important for understanding air-sea interactions and improving satellite measurements of ocean currents, such as those planned by the ODYSEA mission. Traditional methods for measuring near-surface currents, like drifters and HF radars, have limited spatial coverage, while 15 satellite altimetry only captures geostrophic currents, missing high-frequency components like NIOs.

Using a decade-long hourly drifter dataset (2010-2021) and outputs from the high-resolution coupled Ocean/Atmosphere model LLC2160, the study estimates the global spatial decorrelation length scales of NIOs. Drifter pairs were analyzed by latitude and distance, isolating the inertial frequency band. The LLC2160 model, which includes tidal and wind-driven forcing, was validated against the drifter data, showing good agreement in spectral characteristics and correlation scales.

20 Results show that NIO signals have larger decorrelation scales (~105-110 km) compared to low-frequency currents (~70-75 km), with variations by latitude (down to 50 km at high latitudes and near 20°N). These findings suggest that NIO energy is spread over larger spatial scales, linked to atmospheric forcing patterns. The LLC2160 simulation reliably reproduces these spatial characteristics and thus serves as a realistic tool for supporting ODYSEA mission planning.

The study shows that understanding NIO spatial coherency is critical for interpreting satellite Doppler measurements and 25 mitigating aliasing effects, thereby improving ocean current observation capabilities.

1 Introduction

Surface and near-surface currents play an important role in many processes and applications through air-sea interactions (Renault et al., 2016, 2024, Nuijens et al., 2024), transport of drifting material (Onink et al., 2019, van Sebille et al,. 2019), or their impact on sea state (Ardhuin et al., 2017). Today measurements of near surface currents are performed with High-30 Frequency coastal radars (Roarty et al., 2019) or in situ drifters (Lumpkin et al., 2017, Elipot et al., 2016), both with very limited or sparse spatial coverage. These measurements are complemented by indirect estimates of surface currents based on

sea level anomalies using satellite altimetry, combined with an estimate of the mean dynamic topography that also uses a climatology of drifter currents (Mulet et al., 2021). Because these altimeter-derived "geostrophic currents" miss a significant part of the "total surface current", alternative methods are being developed to map surface currents more completely. One approach might be to increase the number of drifters in the ocean. Another promising solution is the perspective of using Doppler radars on satellites (Rodriguez 2018, Ardhuin et al., 2019, Wineteer et al., 2020). Although satellites can provide unprecedented spatial coverage, they can only provide snapshots of the surface current field that contain both low-frequency currents, mostly in geostrophic balance away from the Equator and thus measurable from satellite altimeters, and high-frequency currents with a dominant contribution from the near-inertial frequency band (Yu et al., 2019). Although a long-term average of a sequence of Doppler data can provide useful information, the most novel aspect of this new data is their potential to document the fast-varying and unbalanced components. Early analysis by Ubelmann et al., 2021 suggested that measurements across a 300-km wide swath with a 3-day revisit at mid-latitudes could provide enough constraints to recover more than half of the energy of Near Inertial Oscillations. That analysis was based on modeled currents underestimated NIO velocities and critically relied on the spatial coherence of the NIO velocity field. To better understand the representativeness of in situ or satellite data it is therefore critical to understand the spatial structures of NIOs from actual observations. Although NIOs are generated by winds and are thus expected to contain some large scale pattern (O(1000km)), associated with the large atmospheric Rossby radius. They also respond to the full spectrum of wind patterns and are also known to interact with the ocean mesoscale field potentially resulting in local change of phase and amplitudes.

The ODYSEA (Ocean Dynamics and Sea Exchanges with the Atmosphere) concept mission is a recent satellite mission proposing to measure surface currents and wind stress using a Doppler Scatterometer, over a swath and with a temporal resolution of about 12h at mid-latitudes (Rodríguez et al., 2019; Wineteer, et al., 2020; Torres et al., 2023). The 12h revisit period is not short enough to resolve the period of inertia at mid-latitudes, and the NIO signal may alias the ODYSEA measurements (Wang et al., 2023). Proper characterization of these NIO signals is crucial for a satellite mission like ODYSEA. The aim of this study is therefore to propose a method for estimating a characteristic decorrelation length of the NIO signal in the ocean from the available drifter database. A second objective, in support of future studies for ODYSEA, is to verify that these spatial correlation scales are consistent with simulations from Ocean/Atmosphere coupled models.

To answer these questions, section 2 of this article presents the data from model and in situ and method implemented to estimate the decorrelation length of the NIO signal. The high frequency ocean surface currents are characterized through the analysis of ocean drifting buoy velocities.

Section 3 presents the results obtained from the model and in situ observations focusing on the NIO through their spatial coherency and correlation; and finally, section 4 details the conclusions of this study.

2 Data and Method

2.1 Hourly Surface Velocity Program Drifters

Hourly drifter velocity dataset distributed by the Global Drifter Program (GDP) Data Assembly Center (DAC) (http://www.aoml.noaa.gov/phod/dac/dacdata.php) and described in Elipot et al., 2016 is used. Both velocity at 15m (when drifters are drogued) and at the surface (when the drogue is lost) are provided. The analysis of the high frequency content of this hourly dataset, calculating the globally averaged and zonally averaged anticyclonic and cyclonic rotary spectra of drifter velocities, show that the NIO frequencies can be retrieved. This database has been used extensively to study hight frequency ocean signals, such as the estimation of the wind power on NIO (Liu et al., 2019), the near inertial current (Chaigneau et al., 2008) or Eulerian versus Langrangian currents (Caspar-Cohen et al., 2022; Zhang et al., 2024).

For this study, the amount of data available in the hourly database is low before 2004. So, for computational efficiency and cost, we have limited the time frame of our analysis to a period ranging from 2010 to 2021, which contains most of the data. Both surface (undrogued) and 15m (drogued) drifters are used, but they are analysed separately because undrogued drifters are affected by the direct influence of the wind. Some wind slippage corrections are available, mostly impacting low frequency of the signal (Etienne et al., 2024). We have thus decided to keep the observed surface velocity uncorrected for this study.

2.2 LLC2160-C1440

The outputs of surface current from a numerical model are considered for the statistical comparison of NIO characteristics with what is obtained from the drifters. We chose a simulation from an Ocean/Atmosphere coupled models which should be prone to represent realistic levels of energy for the wind driven current and the NIOs in particular.

The LLC2160-C1440 (Torres et al., 2022 and hereafter LLC2160) simulation is based on the ocean component of the Coupled Ocean-Atmosphere Simulation (COAS) using the Goddard Earth Observing System (GEOS) atmospheric and land model coupled to an ocean configuration of the Massachusetts Institute of Technology general circulation model (MITgcm). The description of the GEOS model can be found in Molod et al., (2015) and Strobach et al. (2020). MITgcm is based on the LatitudeLongitude-polar Cap 2160 (LLC2160) configuration described in Arbic et al. (2018). Horizontal grid is of 2–5 km resolution over the ocean (global horizontal grid spacing of 1/24°) and 7 km for the atmosphere. The vertical grid has 90 levels with thickness ranging from 1m near the surface to 300m below 5000m. This ocean model configuration includes tidal forcing and two-way coupling between winds and ocean currents on wind stresses (Torres et al., 2022) to improve wind and current variability at short time scales. We use here the surface current outputs at hourly frequency of a yearlong simulation (year 2020) as climatological velocity fields. Since both the Atmosphere and the Ocean have a free evolution, we do not expect any particular match between the phases of the drifter and simulation signal, so the comparison will be purely

statistical. For this reason, it was reasonable to consider the run as a statistical realization repeated every year over the longer
95   drifter time extension.

LLC2160 hourly surface data are interpolated onto drifter time and positions whatever the status of the drogue (e.g surface or
15m motion) to provide "Lagrangian-like" LLC2160 trajectories. Hence, in the following, surface currents from LLC2160
are compared to surface and 15m currents derived from drifters, with respect to the spatial and temporal sampling of these
100   observations.
In a recent study, Zhang et al., (2024) demonstrated that in the near-inertial spectral band the Lagangian and Eulerian kinetic
energy (KE) levels are comparable, while Lagrangian KE can underestimate Eulerian KE at tidal and low frequencies.
Hence, using" Lagrangian-like" estimation of the velocity may not affect the LLC2160 comparison to Lagrangian drifter
displacement.

2.3 Selection of pair of drifters and preprocessing

To select pairs of drifters in the near-inertial frequencies, we select drifters in 5° latitude bins. This makes it possible to
obtain trajectories whose time series contain similar inertia frequencies, which depends on latitude. We then select pairs of
buoys that have more than 3 days overlap and isolate the inertial signal, whose periods range from more than 5 days near the
equator to 12 hours at high latitudes. 3 days is a compromise between the number of selected pairs (vanishing when
110   overlapping period increases) and the ability to the Fourier transform tools to separate the entire inertia frequency range.
Hence a low bound of 3 days for the selected time series allows to study NIO excluding only the ±10° around the equator.
When pairs are identified, distance in kilometer between the drifters in a pair is computed. The total number of pairs of
drifters selected in 5° latitude bins are shown in Fig.1. Surface (undrogued) and 15m data (drogued) drifters will sample
different dynamics, as the spatial distribution of the two datasets is different and the surface motion more sensitive to the
115   wind forcing (and more generally to the atmospheric conditions). Basically, undrogued drifters are mainly trapped into
gyres, while 15m drifters follow the main currents. Hence, some basins are sparsely sampled by the drifters, as the Indian
ocean at the surface or south Pacific at 15m (IND and PAC respectively on Fig.1).
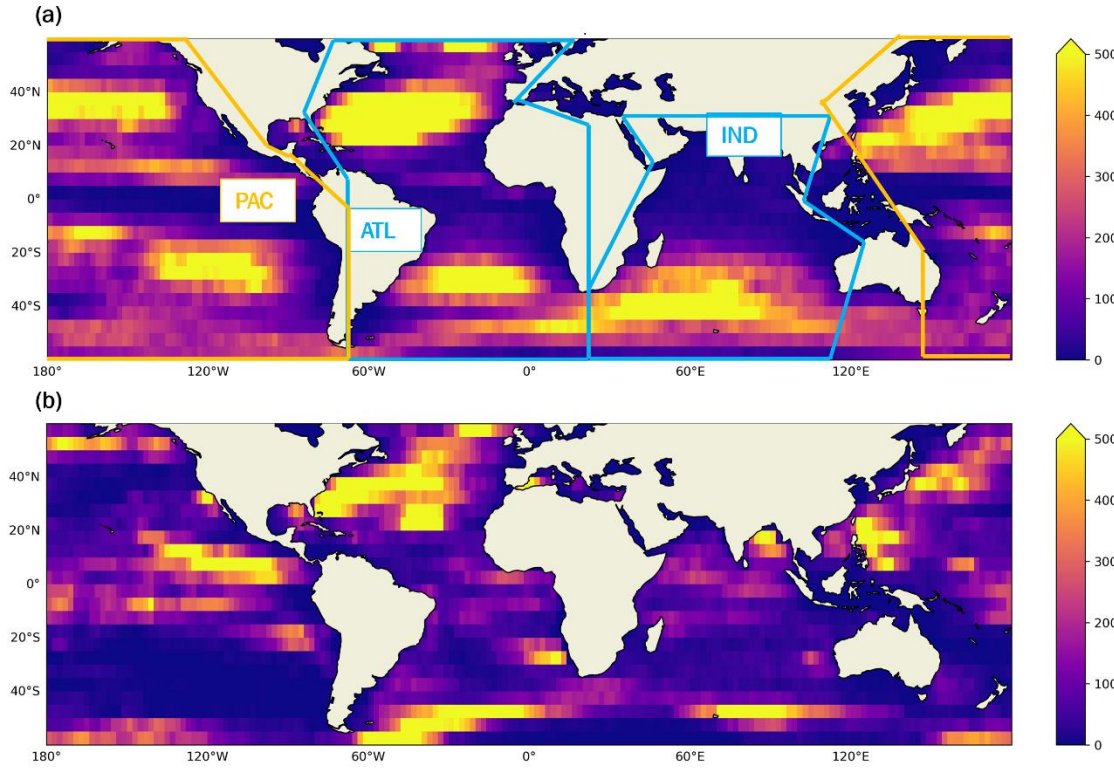
Figure 1: Number of surface (a) and 15m (b) pairs of drifters selected from the hourly SVP data base between January 2010 to
120 **December 2021. Data are binned into 2° longitude x 5° latitude. Regional areas are delimited in blue (ATL for Atlantic Ocean, IND for Indian Ocean) and in orange (PAC for Pacific Ocean).**

2.4 Bandwidth filtering

The inertial period $T_i = 2\pi/f$ depends on the inverse of the Coriolis frequency f. T_i tends toward infinity near the equator and
125 toward 12h at high latitudes. So the higher is the latitude, the higher is the inertial frequency. We chose to apply a Lanczos filter (Duchon 1979) on the drifter trajectories to extract the inertial signal. A bandwidth selection of {0.9f – 1.1f} is applied for each 5° latitude binned drifters of the pairs, with f computed for the mean latitude of the 5° bin. An example of such filter is shown in Fig.2 for two surface drifters of a pair, numbered 1820 in the Pacific Ocean between 45°N and 50°N. Trajectories of the drifters are close together and show a strong NIO event from end of January to mid-February 2015.
130 Inertia loops are clearly seen on Fig.2 (a) and NIO signals are phased during this event (Fig.2 (c)).

In the following, we study both the NIO signal and what we called the "low" frequencies, computed by removing frequencies below 0.9f from the total signal.
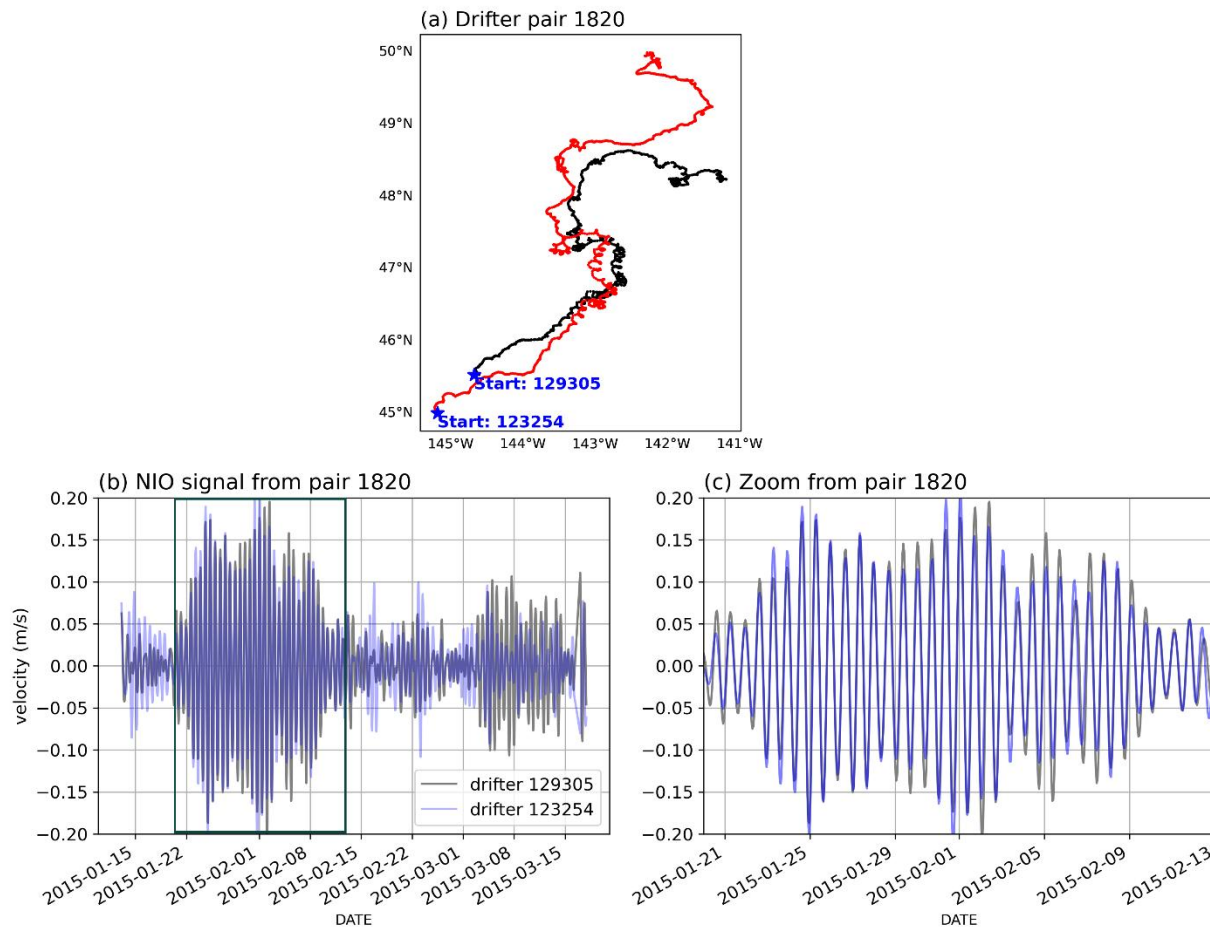
Figure 2: Example of pair numbered 1820 selected between 45° N and 50° N in the Pacific. (a) shows trajectories of the two drifters
135 **129305 and 123254. Times series of the NIO extracted from the zonal velocity on drifter 129305 (black) and 123254 (blue) are**
shown in (b), with a zoom in the black rectangle shown in (c).

2.5 Rotary spectra and correlation between pairs

The globally averaged anticyclonic and cyclonic rotary spectra are computed based on the Elipot et al., (2016) method:
140 trajectories are split into segments of 2160 hours (near 90 days) with 50% overlapping. Then the discrete Fourier transform
of the complex velocity fields (u+iv, where u and v are zonal and meridional velocity, respectively) is computed. In the
following, the rotary spectra are calculated using complete buoy trajectories (and not the selected pairs).

Anticyclonic frequencies (negative in the northern hemisphere, positive in the southern hemisphere) and cyclonic
frequencies (with the opposite sign of anticyclonic) are averaged to obtain a global value. The same method is applied by
145 averaging in 5° latitude bins to observe latitudinal dependencies of the signal variability.

Different diagnostics and statistics based on drifter pairs have been estimated and compared to evaluate their relevance in the estimation of the NIO spatial coherency. We retain here the correlation between drifters of a pair binned by 5km distance. Hence, for each drifter (x,y) of a pair p in a distance bin d, anomaly is computed by removing their respective mean value x_d^p and y_d^p and used to compute the covariance $COV_d(x,y)$, variance $VAR_d(x)$ and correlation $COR_d(x,y)$:

150

$$x_d^p = \frac{1}{Np} \sum_{i=1}^{Np} x_i^p \tag{1}$$

$$COV_d(x,y) = \frac{1}{N} \sum_{p=1}^{P} \sum_{i=1}^{Np} (x_i^p - x_d^p)(y_i^p - y_d^p) \tag{2}$$

$$VAR_d(x) = \frac{1}{N} \sum_{p=1}^{P} \sum_{i=1}^{Np} (x_i^p - x_d^p)^2 \tag{3}$$

$$COR_d(x,y) = \frac{COV_d(x,y)}{VAR_d(x)^{1/2}VAR_d(y)^{1/2}} \tag{4}$$

155

Where N_p the length of the selected time series of pair p in the distance bin d and $N = \sum_{p=1}^{P} N_p$ the total number of data point in the distance bin (sum over the P existing pairs). Hence, we can compute the correlation between drifters of the pairs as a function of their distance, but also as a function of latitude. In this case, pairs are selected in ±2° around the specified latitude (corresponding to a 5° latitude band) and statistics computed every a 1°.

160 **3 Results**

3.1 Assessment of LLC

A first question to be resolved is to which extent the LLC2160 is realistically representing inertial current statistics. Global rotary spectra computed separately on 15m and surface drifters show a better match between surface drifter and LLC2160 (as mentioned in 2.2, only surface currents from LLC2160 are interpolated on surface and 15m drifter data). On Fig.3 (a),

165 surface and 15m anticyclonic rotary spectra are shown. The cyclonic rotary spectrum is not shown here as the NIO is only an anticyclonic motion. Energy level in the surface drifters (grey curves in Fig.3) is systematically higher than at 15m (black curves in Fig.3). Exception can be noticed in the large maximum of surface spectrum between approximately 16h and 30h periods, which is narrower in the 15m rotary spectra. This local flat distribution is the result of the wind-driven inertial oscillations, which is a combination of the variation in the inertia frequency with latitude and the latitudes where the wind is

170 predominant (Elipot and Lumpkin, 2008; Chaigneau et al., 2008). As the effect of wind diminishes with depth, the energy associated with this process should be lower at 15m than at the surface.
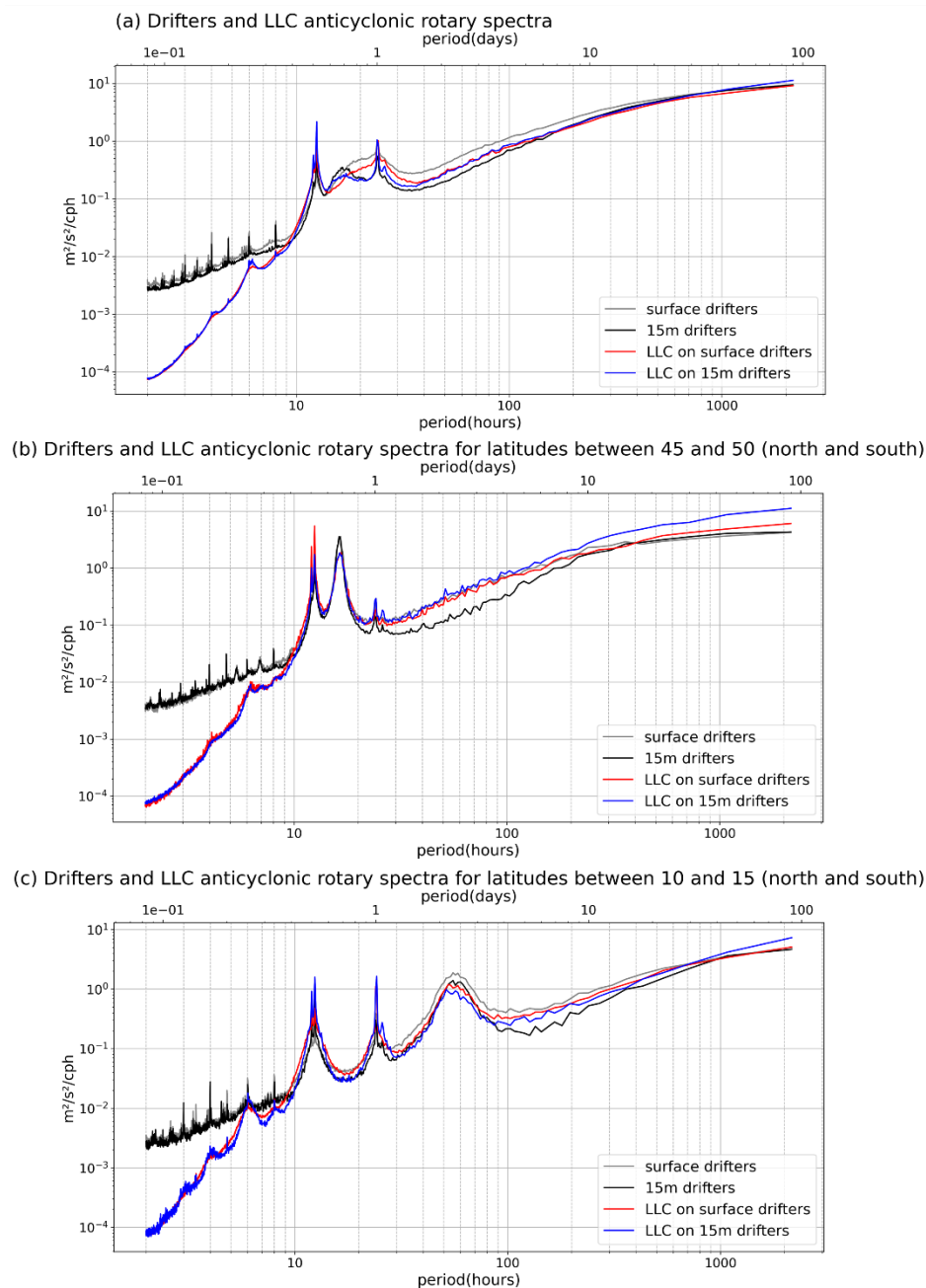
Figure 3: Anticyclonic rotary spectra of surface drifters (grey lines), 15 m drifters (black line), LLC2160 collocated on surface drifters (red) and on 15 m drifters (blue). The global rotary spectra in (a) are the average rotary spectra over the entire domain. (b) are the average rotary spectra between ±45° and ±50°. (c) are the averaged rotary spectra between ±10 and ±15°. Period is expressed in hour (lower axis) and day (upper axis).

175

The global difference in the surface and 15m drifter spatial and temporal distribution (Fig.1) partly explains this exception between the drifter rotary spectra. This point is supported by the LLC2160 spectra, that also differ while the same surface velocity fields (same dynamics) are used for both curves (red and blue in Fig.3).

At short periods (below 10h), the LLC2160 dramatically underestimates the drifter rotary spectra, but this represents only a small proportion of total energy. From the 12h pic maximum and trough the inertia plateau (until period of one day), LLC2160 and drifter curves show the same trend at similar energy level, even if LLC2160 energy is generally weaker than the drifter one (for each distribution respectively). As the minimum period of the inertia is 12 hours (at high latitudes), we can suppose the LLC2160 resolves quite well the NIO frequencies.

The main tidal energy pics (1 day and 12h) are a bit overestimated by the LLC2160. But as stated in Zhang et al., (2024), at tidal frequency Lagrangian spectra is smoother than the Eulerian counterpart, and this result is not critical for this study.

Above 1 day period, the LLC2160 spectra lie between surface and 15m drifter curves, showing an underestimation (overestimation) of the surface (15m) drifter signal respectively. It makes sense considering that the model does not include surface Stokes drift (that nearly disappear in the 15m drifters) but includes a stronger Ekman component than at 15m.

Finally, LLC2160 low frequency signal (i.e. periods greater than 10 days) fairly match the drifter spectra.

If we focus on narrower latitude bands, where the range of NIO frequency is well defined, as in Fig.3 (b) and (c), the inertial peak becomes sharper and LLC2160 still fits quite well the drifter rotary spectra for these frequencies. Between ±45° and ±50°, the inertial period is near 18h (Fig.3 (b)) and near 58h between ±10 and ±15° (Fig.3 (c)). In both cases (and for both 15m and surface distributions), the inertial maximum is clearly displayed in the LLC2160 but remain slightly weaker compared to drifters (by approximately 20%). Finally, we also see a better match between LLC2160 and the surface drifters compared to 15m drifters, especially at low frequencies.

The rotary spectra computed as a function of latitude on Fig.4 brings an interesting global view of the near inertial energy, localized along the white-dotted line. As expected by the integrated spectra of Fig.3, the inertial energy of the LLC2160 simulation is quite consistent with the LLC2160 simulation globally at all latitudes. However, we note a slight underestimation of inertial energy by the LLC2160 simulation a bit more pronounced around 40°N and near the equator. As can be seen on both Fig.3 and Fig.4, the sub-inertial frequency power spectrum is strongly reduced from the surface to 15m, as the surface drifters are submitted to the atmospheric boundary layer with the direct interaction with the wind (surface Ekman layer, waves), while this interaction is decreasing with depth (i.e. Ekman spiral, Stokes drift etc…) For this reason, we will consider in the following only surface statistics.
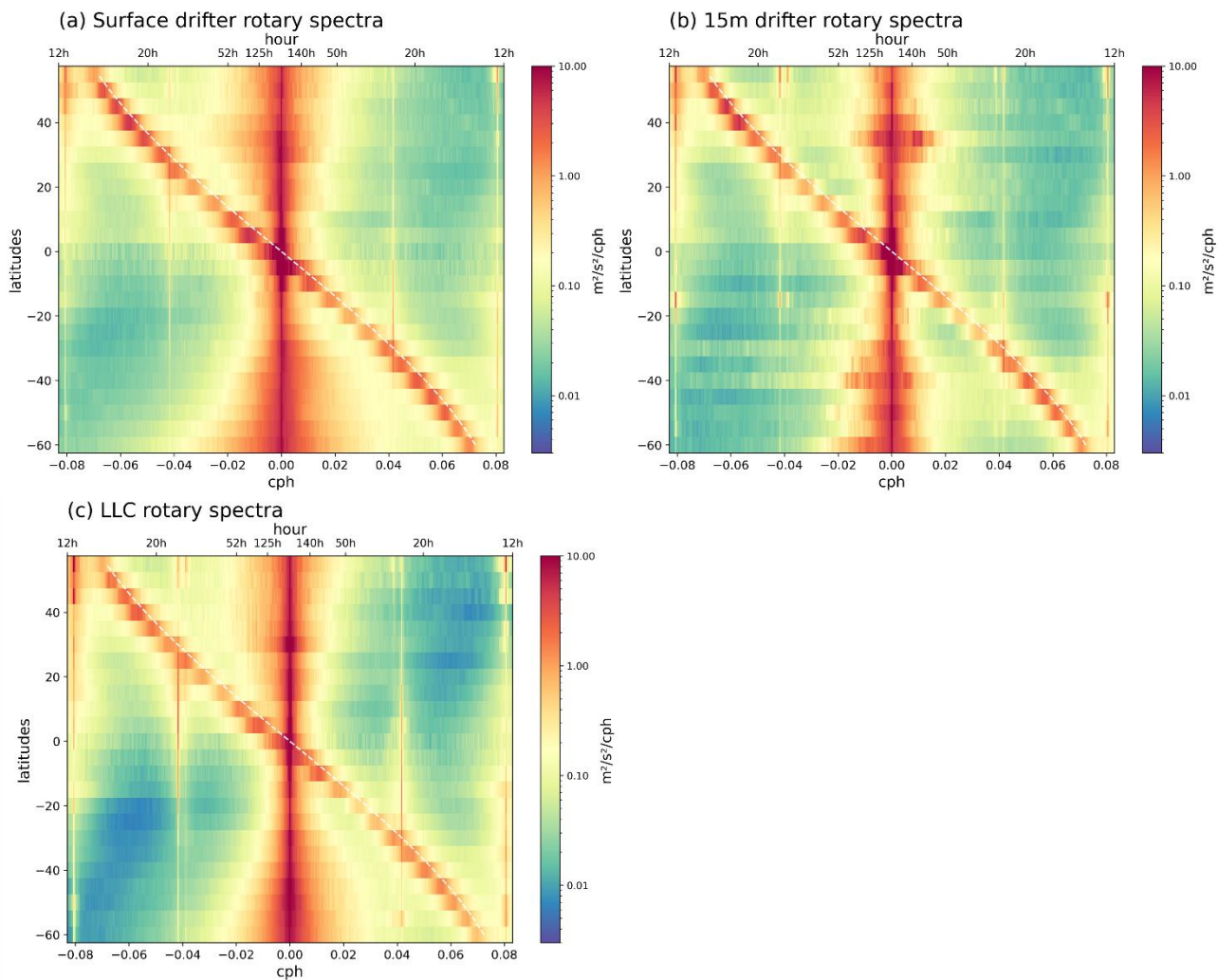
Figure 4: Rotary spectra of surface drifters (a), 15 m drifters (b) and collocated LLC2160 (c) on surface drifters as a function of latitude. Rotary spectra are averaged in 5° latitude bins. Frequency is expressed in cycle per hour (cph) on the bottom axis and respective period in hour is indicated in the top axis. Inertial period is indicated by the white line.

3.2 NIO spatial correlation scale

Correlation between drifter pairs is evaluated following Eq. (4) in 5km bins, using surface drifter datasets. We also show the statistics of the low frequency signal (< 0.9f), extracted from the filtering process as described in 2.4.

The curves of the mean global correlations computed on the surface zonal velocity feature similar characteristics in the drifters and the simulation (Fig.5 (a)). Both low frequencies and NIO correlations match the drifter statistics. The 0.5 threshold for the correlation, that we call the surface decorrelation distance on Fig.5 (b), is reached at 105-110 km for the

NIO, while it is only 70-75 km for the low frequencies. This is an interesting result suggesting that the near-inertial energy is
220   mainly distributed over the wide spatial scales, probably related to the size of atmospheric fronts at first order. At a second
order, there are known interactions between mesoscales and NIO (e.g. Young and Ben-Jelloul, 1997) but they are certainly
not dominant. The NIO energy would remain dominant at the larger scales that of the mesoscales.

However, for distances longer than 300km, the correlations reach a threshold, around 0.2 for low frequencies and 0 for NIO.
This might be explained because low frequencies contain multiple dynamics at many different ranges of spatial scales,
225   including very large ones remaining correlated far beyond 300km.

The surface decorrelation distance from the drifters has a spatial variability (latitude dependency) that LLC2160 correctly
reproduces (Fig.5 (b)). Decorrelation distance of the NIO signal at the surface can reach more than 150 km near the tropics,
down to 50 km at high latitudes (near ±60°) and at 18°N. We do not have a clear explanation for these zonal variations,
probably related to the size of the atmospheric patterns responsible for the inertial energy.

230   For the low frequencies, the match between LLC2160 and the drifters is also very good. We would expect the decorrelation
distance to be related to the Rossby radius size, which seems true from 30°N to 60°N, but not as clear elsewhere.

Over most of the global ocean, NIO and low-frequency signals have different decorrelation scales, which can be used to
differentiate and separate them.
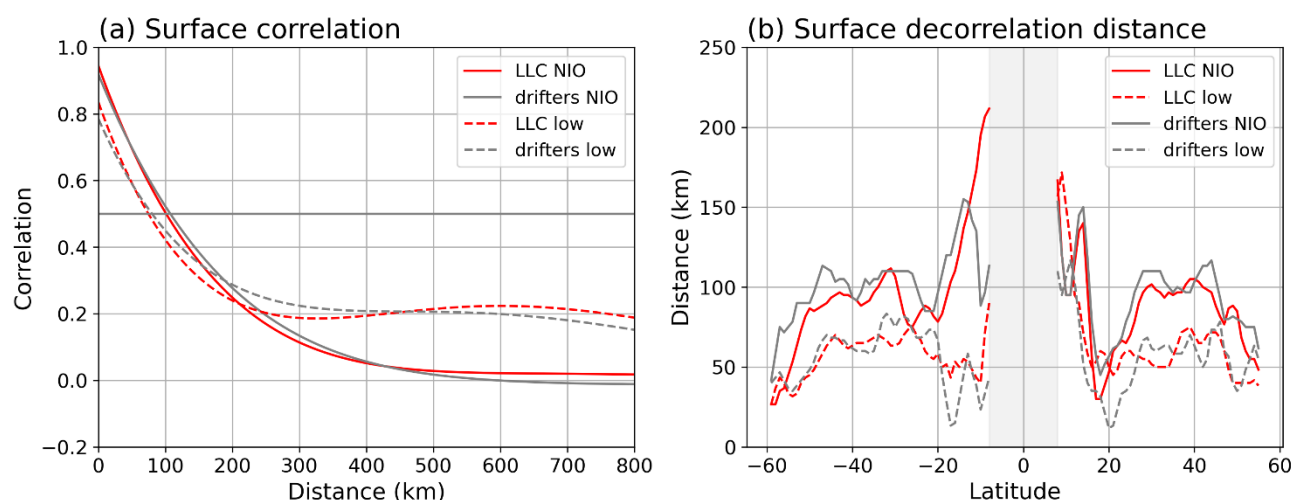
**Figure 5: global surface zonal velocity correlation (a) and surface decorrelation distance (distance at the correlation threshold of
0.5) as a function of latitude (b). Drifter values are plotted in grey and collocated LLC in red. Solid and dash lines indicate values
for NIO and low frequency respectively. In the ±8° region, delimited by the shaded area in (b), signal cannot be properly filtered.**

4 Conclusions

This study successfully characterizes the spatial decorrelation scales of near-inertial oscillations (NIOs) in ocean surface currents using both drifter observations and the LLC2160 coupled ocean-atmosphere model. We have set up a method for

245 characterizing NIO correlation scales. The spatial coherency of the NIO as seen at the surface has been investigated using a 10 years hourly SVP dataset. By selecting pairs of drifters binned by latitude and distance, we have estimated the decorrelation length scale of the NIO, together with the low frequency signal (<0.9f).

The results show that NIOs exhibit larger spatial coherence (~100 km on average) compared to low-frequency currents (Fig. 5 (a)), with significant latitude-dependent variability. The LLC2160 model effectively reproduces the observed NIO spatial

250 patterns and energy spectra, supporting its use in anticipating challenges such as signal aliasing in future satellite missions like ODYSEA, which aims to measure surface currents and wind stress using a Doppler Scatterometer with a 12-hour revisit at mid-latitudes. Thus, LLC2160 constitutes a realistic reference scene for the ongoing ODYSEA studies. More specifically, as suggested in a companion study, the large scales of the NIO patterns can help mitigating aliasing of the ODYSEA signal (S. Jousset personal communication).

255

Data availability :

Hourly drifter observations are produced by Atlantic Oceanographic and Meteorological Laboratory (AOM) of the National Oceanographic and Atmospheric Administation (NOAA). Drifter data can be downloaded from ftp://ftp.aoml.noaa.gov/pub/phod/buoydata/

260 The LLC2160 simulation over year 2020 can be found at https://portal.nccs.nasa.gov/datashare/G5NR/DYAMONDv2/GEOS_6km_Atmosphere-MITgcm_4km_Ocean-Coupled/GEOSgcm_output/geosgcm_surf/

Author contribution:

HE carried out the study and diagnostics. CU, FA and GD supervised the study. HE prepared the article with contributions

265 from CU and FA.

Competing interests:

The authors declare that they have no conflict of interest.

Disclaimer

Acknowledgements: HE and CU acknowledge the French space agency CNES for funding this study and the ODYSEA
270   Science Team for support.

Financial support:

This study has been funded by Centre National d'Etudes Spatiales (CNES) under grant agreement number
ORATSR202402805-ODYSEA

References

275   Arbic, B. K., Alford, M. H., Ansong, J. K., Buijsman, M. C., Ciotti, R. B., Farrar, J. T., Hallberg, R. W., Henze, C. E., Hill,
            C. N., Luecke, C. A., Menemenlis, D., Metzger, E. J., Müeller, M., Nelson, A. D., Nelson, B. C., Ngodock, H. E.,
            Ponte, R. M., Richman, J. G., Savage, A. C., Scott, R. B., Shriver, J. F., Simmons, H. L., Souopgui, I., Timko, P.
            G., Wallcraft, A. J., Zamudio, L., and Zhao, Z.: A Primer on Global Internal Tide and Internal Gravity Wave
            Continuum Modeling in HYCOM and MITgcm, in: New Frontiers in Operational Oceanography, edited by:
280   Chassignet, E. P., Pascual, A., Tintoré, J., and Verron, J., chap. 13, GODAE OceanView, 307–392,
            https://doi.org/10.17125/gov2018.ch13 , 2018.

        Ardhuin, F., S. T. Gille, D. Menemenlis,C. B. Rocha, N. Rascle, B. Chapron,J. Gula, and J. Molemaker: Small-scale open
            ocean currents havelarge effects on wind wave heights,J. Geophys. Res. Oceans, 122, 4500–4517,
            doi:10.1002/2016JC012413, 2017.

285   Ardhuin, F., Chapron, B., Maes, C., Romeiser, R., Gommenginger, C., Cravatte, S., Morrow, R., Donlon, C., & Bourassa,
            M.: Satellite Doppler Observations for the Motions of the Oceans. Bulletin of the American Meteorological
            Society, 100(8), ES215-ES219. https://doi.org/10.1175/BAMS-D-19-0039.1, 2019

        Caspar-Cohen, Z., Ponte, A., Lahaye, N., Carton, X., Yu, X., and Gentil, S. L. : Characterization of internal tide incoherence:
            Eulerian versus Lagrangian perspectives. Journal of Physical Oceanography, 52 (6), 1245-1259, 2022.

290   Chaigneau, A., O. Pizarro, and Rojas, W.: Global climatology of near-inertial current characteristics from Lagrangian
            observations, Geophys. Res. Lett., 35, L13603, doi:10.1029/2008GL034060, 2008.

        Duchon, C. E.: Lanczos Filtering in One and Two Dimensions. Journal of Applied Meteorology, Vol 18, pp 1016-1022,
            1979.

        Elipot, S., and Lumpkin, R.: Spectral description of oceanic near-surface variability, Geophys. Res. Lett., 35, L05606,
295   doi:10.1029/2007GL032874, 2008.

Elipot, S., R. Lumpkin, R. C. Perez, J. M. Lilly, J. J. Early, and Sykulski, A.M.: A global surface drifter dataset at hourly resolution, J. Geophys. Res. Oceans, 121, 2937-2966, doi:10.1002/2016JC011716, 2016

Etienne, H., Verbrugge, N., Boone, C., Rubio, A., Solabarrieta, L., Corgnati, L., Mantovani, C., Reyes, E., Chifflet, M., Mader, J., Carval, T., Guyot, C., Zunino, P.: Quality Information Document, In-Situ Thematic Assembly Centre INSITU_GLO_PHY_UV_DISCRETE_MY_013_044, https://documentation.marine.copernicus.eu/QUID/CMEMS-INS-QUID-013-044.pdf, 2024.

Gonella, J.: A rotary-component method for analysing meteorological and oceanographic vector time series, Deep Sea Res. Ocean-ogr. Abstr., 19, 833–846, 1972.

Liu, Y., Jing, Z. and Wu, L: Wind power on oceanic near-inertial oscillations in the Global Ocean estimated from surface drifters.Geophysical Research Letters, 46,2647–2653. https://doi.org/10.1029/2018GL081712, 2019

Lumpkin, R., T. Özgökmen, and Centurioni,, L.: Advances in the application of surface drifters. *Annu. Rev. Mar. Sci.*, **9**, 59–81, https://doi.org/10.1146/annurev-marine-010816-060641, 2017

Marshall, J., Adcroft, A., Hill, C., Perelman, L., and Heisey, C.: A finite-volume, 495 incompressible navier stokes model for studies of the ocean on parallel computers. 496 Journal of Geophysical Research: Oceans, 102 (C3), 5753-5766, 1997.

Molod, A., Takacs, L., Suarez, M., and Bacmeister, J.: Development of the GEOS-5 atmospheric general circulation model: evolution from MERRA to MERRA2, Geosci. Model Dev., 8, 1339–1356, https://doi.org/10.5194/gmd-8-1339-2015 , 2015.

Mulet, S., Rio, M.-H., Etienne, H., Artana, C., Cancet, M., Dibarboure, G., Feng, H., Husson, R., Picot, N., Provost, C., and Strub, P. T.: The new CNES-CLS18 global mean dynamic topography, Ocean Sci., 17, 789-808, 2021.

Nuijens, L. , J. Wenegrat, P. Lopez-Dekker, C. Pasquero, L. O'Neill, F. Ardhuin, A. Ayet, P. Bechtold, W. Bruch, L.C. Laurindo, X. Chen, F. Desbiolles, R. Foster, I. Frenger, G. George, R. Giesen, E. Hayden, M. Hell, S. Iyer, J. Kousal, N. Laxague, L. Lenain, M.M. Pacheco, A.N. Meroni, S. Minobe, C. Muller, O. O'Driscoll, V. Oerder, N. Pizzo, D. Putrasahan, J.-L. Redelsperger, L. Renault, B. Rommen, C. Sauvage, N. Schneider, M. Shao, P. Siebesma, J. Small, B. Stevens, A. Stoffelen, E. Strobach, P. Sullivan, E.J. Thompson, L. Thompson, I. Uchoa, D. Vandemark, B. Villas Boas, B. Yang, D., S. Zippel: The Air-Sea Interaction (ASI) submesoscale: Physics and impact. Lorentz Center workshop white paper. https://doi.org/10.5065/78ac-qd31, 2024.

Onink, V., Wichmann, D., Delandmeter, P., & van Sebille, E.: The Role of Ekman Currents, Geostrophy, and Stokes Drift in the Accumulation of Floating Microplastic. *Journal of Geophysical Research: Oceans*, *124*(3), 1474–1490. https://doi.org/10.1029/2018JC014547, 2019

Renault, L., M. J. Molemaker, J. C. McWilliams, A. F. Shchepetkin, F. Lemarié, D. Chelton, S. Illig, and A. Hall : Modulation of Wind Work by Oceanic Current Interaction with the Atmosphere. *J. Phys. Oceanogr.*, **46**, 1685–1704, https://doi.org/10.1175/JPO-D-15-0232.1, 2016

Renault, L., Arsouze, T., Desbiolles, F. et al. Rectification effects of regional air–sea interactions over western boundary current on large-scale sea surface temperature and extra-tropical storm tracks. *Sci Rep* **14**, 31771 https://doi.org/10.1038/s41598-024-82667-2, 2024.

Rio, M.-H., and Hernandez, F.: High-frequency response of wind-driven currents measured by drifting buoys and altimetry over the world ocean, J. Geophys. Res., 108(C8), 3283–3301, doi:10.1029/2002JC001655, 2003.

Roarty, H., Cook, T., Hazard, L. et al.: The Global High Frequency Radar Network. Frontiers in Marine Science, 6. 00164. ISSN 2296-7745 https://doi.org/10.3389/fmars.2019.00164, 2019.

Rodríguez, E.: On the optimal design of Dopplers catterometers. *Remote Sensing*, **10**(11), 1765. https://doi.org/10.3390/rs10111765, 2018

Rodríguez, E, Bourassa, M., Chelton, D., Farrar, J. T. , Long, D. , Perkovic-Martin, D. and Samelson, R.: The Winds and Currents Mission Concept, *Frontiers in Marine Science,* **6**, https://www.frontiersin.org/articles/10.3389/fmars.2019.00438, 2019.

van Sebille, E., Delandmeter, P., Schofield, J., Hardesty, B. D., Jones, J., and Donnelly, A.: Basin-scale sources and pathways of microplastic that ends up in the Galápagos Archipelago, Ocean Sci., 15, 1341–1349, https://doi.org/10.5194/os-15-1341-2019 , 2019.

Strobach, E., Molod, A., Trayanov, A., Forget, G., Campin, J.-M., Hill, C., and Menemenlis, D.: Three-to-Six-Day Air–Sea Oscillation in Models and Observations, Geophys. Res. Lett., 47, e2019GL085837, https://doi.org/10.1029/2019GL085837 , 2020.

Torres, H. S., Klein, P., Wang, J., Wineteer, A., Qiu, B., Thompson, A. F., Renault, L., Rodriguez, E., Menemenlis, D., Molod, A., Hill, C. N., Strobach, E., Zhang, H., Flexas, M., and Perkovic-Martin, D.: Wind work at the air-sea interface: a modeling study in anticipation of future space missions, Geosci. Model Dev., 15, 8041–8058, https://doi.org/10.5194/gmd-15-8041-2022 , 2022.

Torres, H., Wineteer, A., Klein, P., Lee, T., Wang, J., Rodriguez, E., Menemenlis, D. and Zhang, H.: Anticipated capabilities of the ODYSEA wind and current mission concept to estimate wind work at the air–sea interface. *Remote Sensing*. **15**(13):3337. https://doi.org/10.3390/rs15133337, 2023

Ubelmann, C., Dibarboure, G., Gaultier,L., Ponte, A., Ardhuin, F., Ballarotta, M.,& Faugère, Y.: Reconstructingocean surface current combiningaltimetry and future spaceborneDoppler data. Journal of GeophysicalResearch: Oceans, 126, e2020JC016560.https://doi.org/10.1029/2020JC016560, 2021.

Wang, J., Torres, H., Klein, P., Wineteer, A., Zhang, H., Menemenlis, D., Ubelmann, C., and Rodriguez, E.: Increasing the observability of near inertial oscillations by a future ODYSEA satellite mission, *Remote Sensing, 15*(18), 4526. https://doi.org/10.3390/rs15184526, 2023

360 Wineteer, A., Torres, H. S., and Rodriguez, E.: On the surfacecurrent measurement capabilities of spaceborne Doppler scatterometry.Geophysical Research Letters,47, e2020GL090116. https://doi.org/10.1029/2020GL090116, 2020.

Young, W. R., and Mahdi B. Jelloul: Propagation of near-inertial oscillations through a geostrophic flow. Journal of Marine Research 55, (4). https://elischolar.library.yale.edu/journal_of_marine_research/2242, 1997.

Yu, X., Ponte, A. L., Elipot, S.,Menemenlis, D., Zaron, E. D., and Abernathey, R: Surfacekinetic energy distributions in
365 theglobal oceans from a high-resolutionnumerical model and surface drifterobservations. Geophysical ResearchLetters, 46, 9757–9766. https://doi.org/10.1029/2019GL083074, 2019.

Yu, X., Naveira Garabato, A. C., Vic, C., Gula, J., Savage, A. C., Wang, J., Waterhouse, A. F., and MacKinnon, J. A.: Observed equatorward propagation and chimney effect of near-inertial waves in the midlatitude ocean. Geophysical Research Letters, 49, e2022GL098522. https://doi.org/10.1029/2022GL09852, 2022.

370 Zhang, X., Yu, X., Ponte, A. L., Caspar-Cohen, Z., Le Gentil, S., Wang, L., Gong, W : Lagrangian Versus Eulerian Spectral Estimates of Surface Kinetic Energy Over the Global Ocean, J. Geophys. Res., 109(C8), doi: 10.1029/2024JC021057, 2024